



An experimental investigation on lateral crushing response of glass/carbon intraply hybrid filament wound composite pipes

Özkan Özbek¹ · Nurettin Furkan Doğan¹ · Ömer Yavuz Bozkurt²

Received: 7 April 2020 / Accepted: 25 June 2020 / Published online: 3 July 2020
© The Brazilian Society of Mechanical Sciences and Engineering 2020

Abstract

The current study aimed to examine an experimental investigation on the energy absorption capability of glass/carbon intraply hybrid filament wound composite pipes subjected to quasi-static lateral compression loading. The composite pipes with different fiber orientation angles were fabricated for both hybrid and non-hybrid to systematically analyze the performance of intraply hybridization process. At least 5 samples of each composite pipe configuration were tested to obtain the load–displacement curves and fracture patterns. The failure modes and fracture mechanisms of crushed samples were discussed to establish the influence of hybridization on crashworthiness parameters through load–displacement response. Separation between the layers (delamination) was occurred as the main damage mechanism in all samples. Hybridization with glass fiber significantly increased the energy absorption capability and load carrying capacity of carbon fiber-reinforced composite pipes. Their crushing values were found as between the values of pipes made of glass fiber and carbon fiber as expected. Furthermore, hybridization provided to opportunity of more stable load–displacement response for crushing process. An increment in fiber orientation angle was also led to increase in energy absorption capability and load carrying capacity. The pipe made of glass with higher fiber orientation had the best specific energy absorption.

Keywords Intraply fiber hybridization · Lateral crushing · Filament winding

1 Introduction

The use of thin-walled composite structures, featuring high strength and lightweight in high tech-industries such as aerospace, defense, automotive and marine, has become one of the most distinctive and promising structural component forms to improve overall performance by reducing mass and cost. The use of composite materials in those industries is generally based on the superior strength-to-weight ratio, high corrosion resistance, promising fatigue life and better vibration-damping characteristics compared to those of conventional monolithic engineering materials [1–3]. In recent years, passenger vehicle industry is facing difficulties

in meeting the requirements of new or changing regulations on safety standards and emission legislations with the use of traditional metallic structural materials. These challenges have brought up the use of composite materials for the development of crashworthy structures in vehicles through the absorption of impact energy in a controlled manner during an impact event. In this regard, in spite of their brittle nature, composite materials with proper design have also been proposed as a superior alternative to classical metallic-based engineering materials like steel and aluminum [4, 5] and are stated as significant structural energy absorbing components for the possible impact events [6].

Composite materials have popularly used in different structural forms such as beams, columns, plates, shells, tubes, etc. and a great number of scientific studies related with the mechanical, dynamical and thermal properties of composite materials are found in the literature [7–13]. A certain part of these researches has been devoted to the mechanical properties of composite pipes and especially focused on filament wound composite pipes. The most common properties investigated are burst performance [14, 15], tensile and compressive characteristics [16–19], fatigue

Technical Editor: João Marciano Laredo dos Reis.

✉ Özkan Özbek
ozkanozbek@kilis.edu.tr

¹ Mechanical Engineering Department, Kilis 7 Aralık University, 79000 Kilis, Turkey

² Mechanical Engineering Department, Gaziantep University, 27310 Gaziantep, Turkey

behavior [20–22] and impact response [23–25]. Gemi et al. [26] analyzed the effects of various drill types on drilling performance of glass fiber-reinforced composite pipes. Drilling experiments were assessed for 5000 rpm spindle speed and different feed rate parameters such as 25, 75, 125, 175, 225 and 275 mm/min. Rafiee et al. [16] performed experimental and numerical investigations on the damage progression and the failure mechanism of glass fiber-reinforced pipes under transverse compressive loading. The level of diametric deflection at which failure beginning was determined, and simulations using FE analysis were evaluated for intralayer and interlayer failures. A good agreement between experimental and numerical observations was observed, and progress of damage was studied for various diametric deflection levels. Maleki et al. [27] examined the influence of geometrical parameters, in terms of delamination size and its position, on the stiffness of composite pipes subjected to compression loading in accordance with ASTM D2412 standard. Using cohesive zone method, FE analysis was used to simulate behaviors of pipes. It was stated that the existence of delamination which depends on size, at the interface of adjacent layers resulted with reduction in stiffness values of pipes. In the literature, numerous studies have been devoted to the crashworthiness of composite materials [28–30]. However, despite the importance of the crushing response of the structure under low-velocity lateral impact for passenger safety in various passenger vehicles [31], most of these studies have mainly focused on crushing properties under axial compression load [32–35], and the limited number of studies has been carried out on the lateral crush response of polymer-based composite materials. The lateral compression studies have dealt with the factors that affect the crashworthiness of a material such as cross-sectional geometry [36, 37], fiber types [6, 38], fiber orientation angle [38, 39] and filler material [4, 40, 41]. Among them, due to its decisive influence on the failure mechanisms and the crushing modes, the fiber reinforcement type has a crucial role on the crashworthiness. Abosbaia et al. [42] investigated the effects of segmentation on the lateral crushing response of the laminated composite tubes reinforced by carbon fiber, cotton fiber and glass fiber. It was stated that low energy absorption levels of the lateral crushing caused from the unstable load–displacement response of the materials. Also, efficient crush responses of carbon and cotton fiber-reinforced samples were reported. Sebaey et al. [36] examined the crashworthiness of hybrid hexagonal/octagonal cellular composites made of carbon/epoxy fiber reinforcement by laterally compressing at 5 mm/min crosshead speed. The samples having closed cells showed the better peak load, mean crushing loads and energy absorption, while worse in stability of load–displacement response compared to open cells samples. Sari et al. [43] assessed the residual failure pressures and fatigue life of composite pipes subjected to

lateral impact. Samples having glass fiber reinforcement with $\pm(55^\circ)_6$ winding angle were exposed to three different energy levels for impact tests. They revealed that failure pressure of non-impacted pipe has higher than the impacted one at 5.0 J energy level about 34% and 40%. Hafeez and Almaskari [44] carried out an experimental fiber or study related to scaling laws in laterally indented filament wound tubes supported with V-shaped cradles. The scaling factors of the tubes having glass fiber reinforcement and epoxy matrix were determined by using Buckingham Pi theorem for geometric dimensions of the samples. Abdewi et al. [37] analyzed the effect of corrugation cross-sectional geometry on the crashworthiness of woven roving glass fiber-reinforced laminated composite tubes. It was reported that the samples subjected to lateral compression was not influenced by corrugation geometry and was fractured due to formation of longitudinal fracture lines. Li et al. [45] performed an experimental and numerical studies devoted to comparison of lateral crushing responses of circular aluminum, carbon fiber-reinforced pipes (CFRP) and glass fiber-reinforced pipes (GFRP) subjected to lateral compression loading. It was seen that the aluminum pipes exhibited the best lateral crashworthy performance due to its ductile characteristics. It was also reported that GFRP exhibited marginally better performance than CFRP samples.

To the best knowledge of authors to date, there is no published work in the open literature on the lateral crushing characteristics of glass-carbon intraply fiber-reinforced filament wound composite pipes. Hence, the motivation of the present work is to experimentally evaluate the influence of intraply glass fiber hybridization on the crashworthiness performance of carbon fiber-reinforced filament wound composite pipes in terms of energy absorption, peak and mean crushing loads, specific absorbed energy and failure modes. In order to gain a better insight into the influence of intraply hybridization on the lateral crushing, the samples with different fiber orientation angles ($\pm(40^\circ)_6$, $\pm(55^\circ)_6$, $\pm(70^\circ)_6$) and six layers were also prepared and subjected to quasi-static compression loadings, laterally. The energy absorption, peak and mean crushing loads, specific absorbed energy and failure modes of hybrid samples were comparatively analyzed with those of non-hybrid ones.

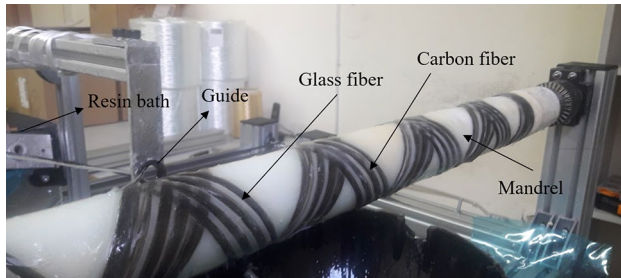
2 Materials and method

2.1 Materials

Glass fiber roving of 2.4 K tex (Plasto A. Ş., Turkey), carbon fiber roving of 12 K tex (Dost Kimya A. Ş., Turkey), EPIKOTE MGS LR160 resin (Dost Kimya A. Ş., Turkey), and EPIKURE MGS LH260S Curing Agent (Dost Kimya A. Ş., Turkey) were used for the reinforcement and matrix

Table 1 Mechanical and physical properties of the constituents

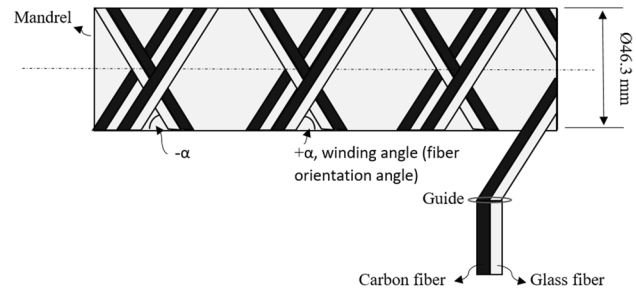
Material	Tensile strength (MPa)	Tensile modulus (GPa)	Elongation at break (%)	Filament diameter (μm)	Specific density (g/cm^3)	Size content (%)
Glass fiber	1970	79	3.5	17	2.56	0.55 ± 0.15
Carbon fiber	3950	238	1.5	7	1.77	1.25 ± 0.25
Epoxy (neat)	70–80	3.2–3.5	5.0–6.5	–	1.18–1.20	–

**Fig. 1** Filament winding process (glass/carbon intraply fiber hybridization)

system of composite pipe samples. The mechanical and physical properties of the constituents were given in Table 1.

2.2 Sample fabrication

A wet filament winding technique was used to fabricate all considered samples. The fabrication process of fiber-reinforced composite pipes can be categorized into three distinct steps as preliminary preparations, winding procedure and curing process. Firstly, release wax was applied on the mandrel and release agent film was wrapped. Afterward, release wax was again implemented on the release agent film to easy pull out the mandrel from the pipe at the end of the winding process. The glass wool was implemented to obtain smooth surface on inner surface of the pipe samples. Resin tank was filled with the resin system (a mixture of epoxy and hardener) to wet the fiber reinforcements. Fiber reinforcements were connected to the mandrel by passing through the tank with a series of rollers guide placed in front and behind the resin tank. After the preliminary preparations were completed, the filament winding process was started by uploading the required motion codes to the machine. A bundle of direct roving comprising of 2 strands with a certain bandwidth is impregnated with unsaturated epoxy resin and then wound around mandrel (bandwidths: 3.8 mm for glass fiber, 3 mm for carbon fiber). Carbon and glass fibers were simultaneously wound onto the mandrel in the desired orientation angle as shown in Fig. 1. In the curing stage, composite pipe preform was wrapped with a heat shrink tape and left to cure at room temperature for 24 h. Following the

**Fig. 2** Schematic illustration of intraply fiber hybridization

curing, the composite pipe was exposed to heat at $40\text{ }^{\circ}\text{C}$ for 2 h to perform post-curing process.

Fiber hybridization is one of the promising strategies to tailor the properties of composite materials [46]. Interply and intraply are two different fiber hybridization structures that are commonly used in the literature [28, 47]. Interply fiber hybridization is based on the use of different fiber materials in different layers of composite laminate, while intraply fiber hybridization is based on the use of different fiber reinforcements in the same layer. The intraply fiber hybridization, by co-winding of glass and carbon fiber reinforcements at the same layer, as shown in Fig. 2, has been employed in this study. All manufactured hybrid and non-hybrid composite pipe samples were composed of six layers with constant winding angles of $\pm(40)_6$, $\pm(55)_6$, and $\pm(70)_6$.

The examples of hybrid and non-hybrid pipe samples were shown in Fig. 3 and the detailed information like naming, fiber mass fractions, mass and thickness, were presented in Table 2. The length and inner diameter of all the samples are the same and are equal to 170 mm and 46.3 mm, respectively. To determine fiber mass fractions, ignition loss experiments were conducted in accordance with the ASTM D2584 standard [48].

2.3 Lateral compression tests

A computerized servo universal testing machine (Shimadzu AG-X Series) having a frame capacity of 300 kN was used to determine the lateral crushing properties of the samples. The experimental tests were performed as a continuation of stiffness tests based on ASTM D2412 standard [49] which is a useful source to examine stiffness characteristics of

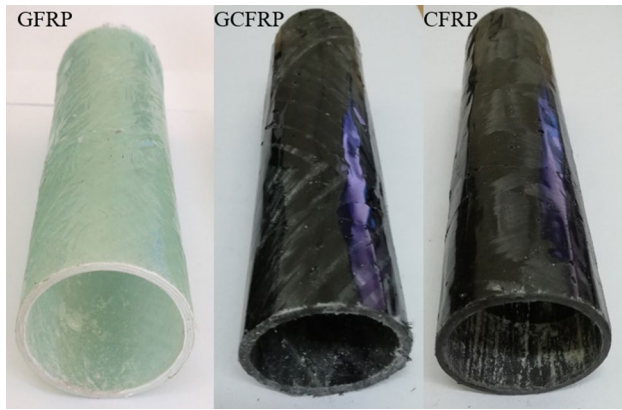


Fig. 3 Samples for lateral compression test

plastic pipes in lateral direction. The lateral compression tests were carried out by compressing the sample between two flat platens (one stationary and one moving) at a constant crosshead speed of 12.5 mm/min until 75.6% diametric deflection (35 mm stroke), as seen in Fig. 4. After that value, the compression loading were stopped owing to the beginning of densification phase which implies load values increase sharply caused by almost complete compaction of tested pipe. During the test procedure, the load–displacement curve and the photographs of samples at different compression stages were recorded to follow the crushing process. The tests were repeated for at least five samples of each composite configuration and the values were averaged.

In general, the materials showing the brittle nature have the three main stages as pre-crushing, post-crushing and densification entire the crushing process [50]. Pre-crushing stage, also called as elastic region, is directly related to safety protection of the occupants. Only initial peak load should be noted to understand which crushing event are happening (catastrophic or progressive) by comparing with mean crushing load. Crashworthy phenomenon is concerned with post-crushing is started with small inter- or intralaminar cracks nucleating with local stress concentration immediately after the initial peak load point. Lastly, material densification begins where the load increases sharply. The crashworthiness parameters of composite materials are calculated as follows:

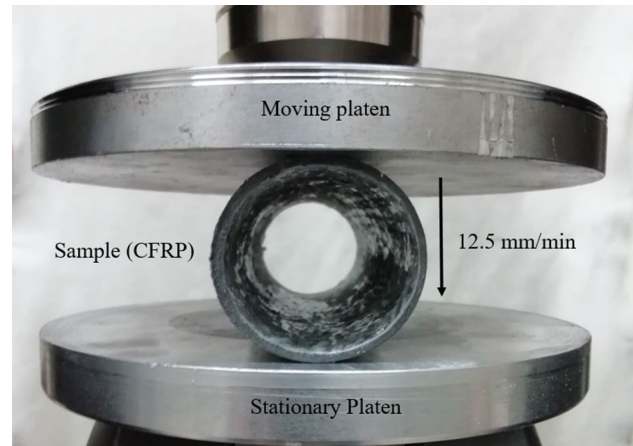


Fig. 4 The lateral compression test

Total energy absorption, E , is the area under load–displacement curve between crush distances and is calculated by integration of load, P , as seen Eq. (1);

$$E = \int_{S_i}^{S_f} P(s)ds \tag{1}$$

where S_i and S_f represents the initial and final stroke values in post-crushing stage, respectively. Also, mean crushing, P_m , load is obtained from the integration of each load value depending on stroke, $P(s)$ as in Eq. (2);

$$P_m = \frac{\int_{S_i}^{S_f} P(s)ds}{S_f} \tag{2}$$

Crushing load efficiency, η_f , which is a measure of the crushing process stability, is the ratio of mean crushing load per initial peak load and is calculated as follows,

$$\eta_f = 100(P_m/P_i) \tag{3}$$

where the peak load (P_i) is the initial peak load in the load–displacement curve.

Specific energy absorption, E_s , is one of the crucial parameters that evaluates crushing characteristics of a structure taking its mass into consideration. Simply, it is

Table 2 Naming, thickness, mass and fiber amounts of filament wound composite pipes

Fiber/epoxy composite pipes	Naming	Number of plies	Thickness (mm)	Mass (g)	Fiber mass fraction (wt%)
Glass/epoxy FRP	GFRP	6	3.67 ± 0.08	108.4 ± 5.0	71.5 ± 0.25
Glass-carbon/epoxy FRP	GCFRP	6	3.25 ± 0.07	93.8 ± 7.5	53.8 ± 0.90
Carbon/epoxy FRP	CFRP	6	2.58 ± 0.08	63.5 ± 3.5	56.9 ± 0.32

the absorbed energy per unit mass of crushing sample and is calculated as follows,

$$E_s = \frac{E}{m_{\text{crush}}} = \frac{\int_{S_i}^{S_f} P(s) ds}{m_{\text{crush}}} \quad (4)$$

3 Results and discussions

3.1 Load–displacement history and failure modes

The load versus displacement curves and the crushing history of the lateral loading application at different fiber orientation angles of the hybrid and non-hybrid composite pipes were given in Figs. 5 and 6, respectively. For the all examined samples, mid-surface of samples were observed as damage region beginning with a behavior of buckling of the vertical walls encouraged by delamination [27]. This buckling allowed and encouraged the cells to readjust its position which causes a vertical crack at the samples mid-plane [6]. Furthermore, first failure mode can be given as matrix cracking that triggers delamination of the layers. Most of the samples showed the fiber debonding failure mode by splaying outward as lateral loading continued. Furthermore, progressive collapse was observed from all considered samples.

The load–displacement curves of the samples having the considered fiber orientations were given in Fig. 5a–c, respectively. There were irregular ups and downs in the graphs, caused from individual breaks in each layer. The sudden drops in loads were caused from delamination evolution that results with energy dissipation as a result of damage process [27]. They were associated with delamination failures due to damage initiation [51, 52]. As the surface contact with the load was worse than the cross-sectional flatness, cyclic load–displacement graphs could not be obtained as in axial crush. CFRP had the lowest load carrying capacity because of its thinner structure. Also, higher fiber orientation angle resulted with the increase in load carrying capacity as reported in İsmail's study [38]. GFRP with $\pm(70^\circ)$ fiber orientation had the maximum initial loading peak value and the most regular curve for the crushing application. Hybridization process fixed the unstable behavior of the GFRP response that shows the irregular load–displacement. Furthermore, the area under curve of the CFRP was increased by fiber hybridization.

The crushing histories of the samples with the fiber orientation of $\pm(40^\circ)$, $\pm(55^\circ)$ and $\pm(70^\circ)$ were presented in Fig. 6a–c, respectively. For all samples, the separation between layers (delamination) after matrix fragmentation was seen as predominant failure mode particularly in GFRP and GCFRP samples. These delamination failures were formed in adjacent hoop layers that all layers separated

from each other [16]. Similar findings were obtained from a comparison study devoted to lateral crushing of aluminum, GFRP and CFRP pipes performed by Li et al. [45]. It was also reported that delamination failures were the main failure mode for thicker composite pipes (GFRP), indicating the more energy absorption through the delamination failure. The fiber breakage was followed the delamination layer by layer. Additionally, stable lateral crushing process with buckling was obtained. The standard stable failure process as change in cross section from circular to elliptical was happened on all samples [53]. Fiber debonding as failure mode was seen on samples in mostly since weak interfacial adhesion between layers, especially in intraply ones.

After crushing application, the samples returned back a certain amount because of spring back effect. But they did not take the original circular characteristics shapes due to plastic deformation and failure inside the samples. The damaged appearances of the hybrid and non-hybrid samples were given in Fig. 7 as front and top views. The macro- and micro-damages were monitored using a high-resolution camera and a microscope, respectively. It is seen that with the loading of pipes the top and bottom sides contacted with platens are initially flatten out, and the left and right sides bend outward. This has led to tension stress at outer surfaces of left and right sides, and tension stress at inner surfaces of top and bottom sides. When the local stresses at the outer surface of left and right sides are started to exceed the stress capacity, the matrix cracking failures were occurred on them. A further increase in load caused inward bending of top and bottom sides. The bending of right-left (outward) and top–bottom (inward) sides caused to tensile/compression stress developments at inner and outer surfaces which were led to different stress levels at different layers. Afterward, delamination between layers began and the separation of layers was observed obviously in four regions of samples as top, bottom, left and right. Hamouda et al. [37] also reported much more evident delamination on the same regions compared to other sections. It is believed that the sudden drops in load–displacement curves are the result of delamination which is evaluated as a kind of energy dissipation mechanism in composite materials. The formation of delamination which means separation of layers at circumferential direction led to decrease in load bearing capability due to reduction in stiffness of the samples [27]. Therefore, the load-deformation has displayed a linear behavior until separation of layers began. Delamination (interlaminar damage) has occurred as the major mode of failure. Furthermore, it is seen that the delaminated regions at inner surface were larger than that of outer surface, and the matrix cracking was more dominant at outer surface compared to the delamination. Similar findings were also reported by Gemi [7] in a study devoted to

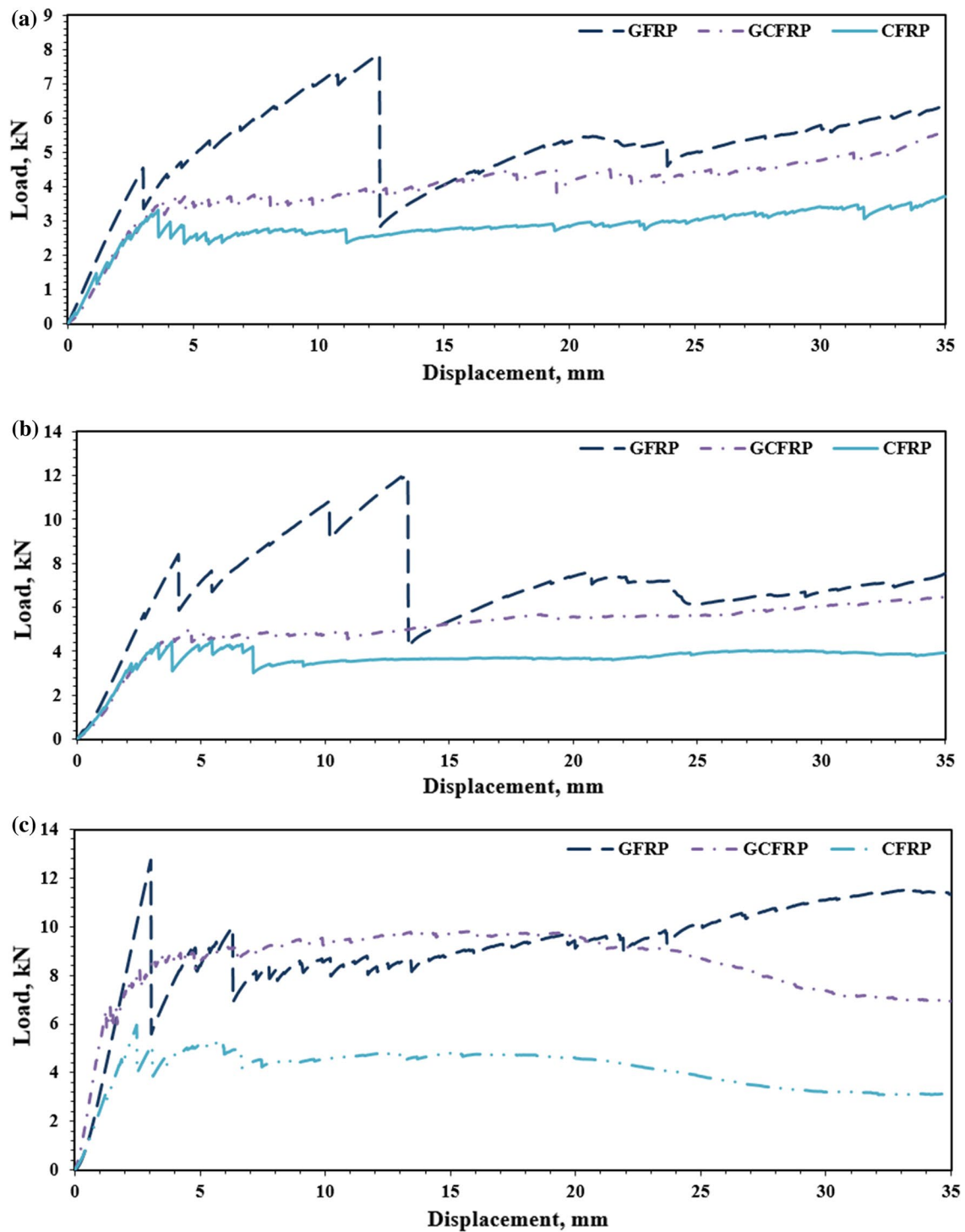


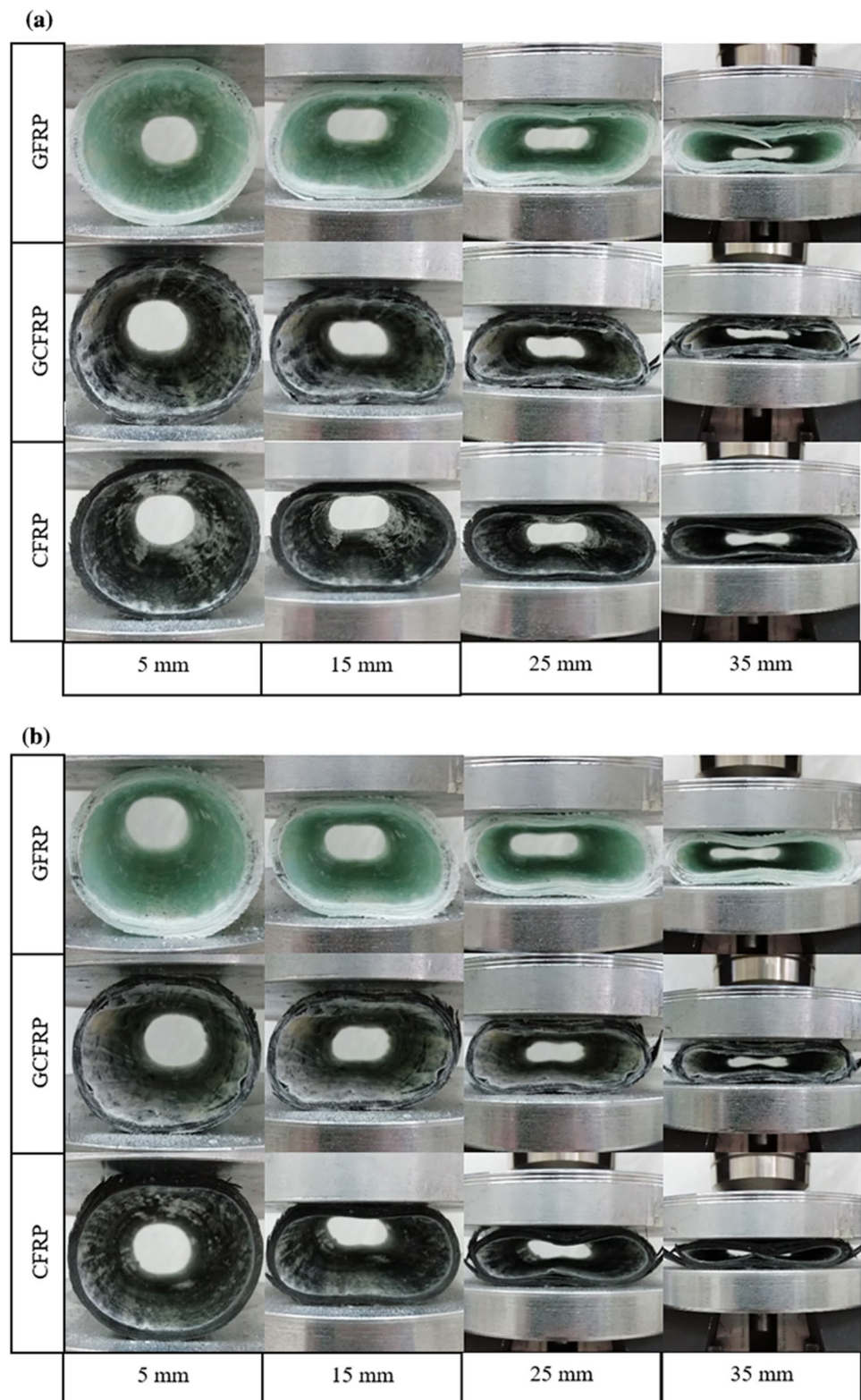
Fig. 5 Load-displacement responses for **a** $\pm(40^\circ)_6$ fiber orientation, **b** $\pm(55^\circ)_6$ fiber orientation, **c** $\pm(70^\circ)_6$ fiber orientation

effect of stacking sequences on the low velocity impact and damage formation in hybrid composite pipes. It was informed that the compression/tension stress at the outer surface resulted with matrix cracking mostly while the tensile stress at inner layers was caused the matrix cracking/

delamination failures. Also, the formation of delamination was ascribed to shear stresses caused by bending phenomena in transverse direction.

The regions, where the separation of layers occurred, are the beginning of longitudinal fiber fracture lines triggered

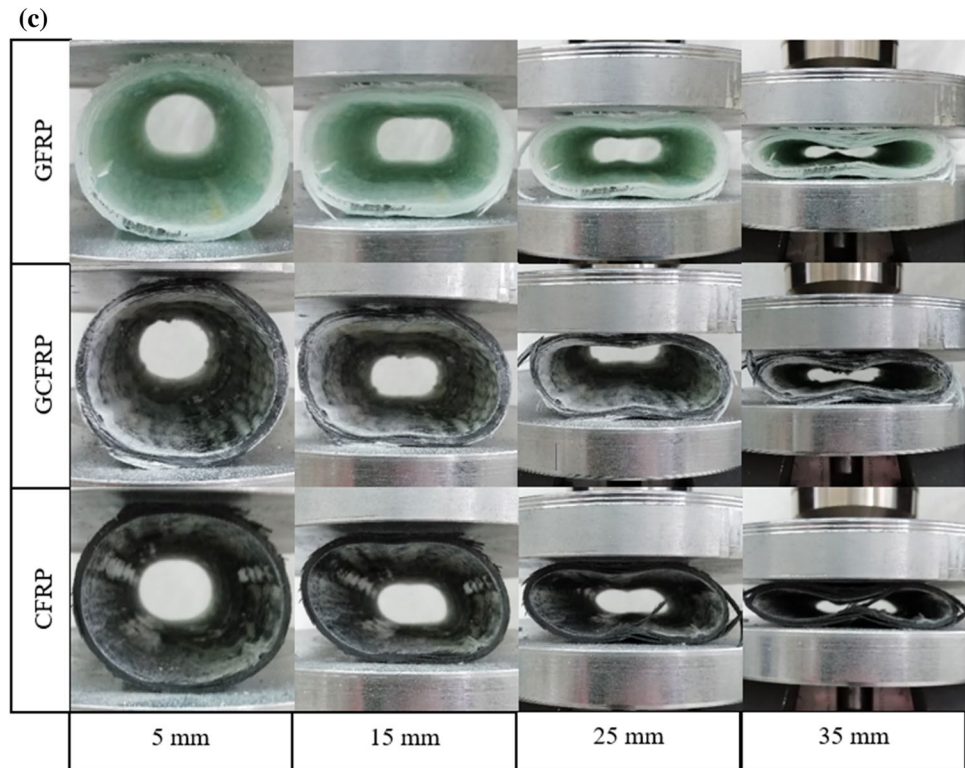
Fig. 6 Crushing histories; **a** $\pm(40^\circ)_6$ fiber orientation, **b** $\pm(55^\circ)_6$ fiber orientation, **c** $\pm(70^\circ)_6$ fiber orientation



by fiber debonding intensification. As the increase in compression continued, longitudinal fiber cracks especially in the left and right side of samples were formed due to much more delamination. Madenci et al. [12] reported a similar

finding that the intense of matrix cracking and debonding damage areas ended with fiber fractures and fiber pull-out damage formations. Abosbaia et al. [42] also found parallel results, reporting the crack propagation on the diametrically

Fig. 6 (continued)



opposite sides with a right angle from the contact lines with platen as the main reason for sharp drop-off in loads which means little energy absorption in the crushing process.

In summary, the failure process initiated with the matrix cracking and followed with delamination. Fiber breakage failures were generally achieved as longitudinal cracks which happened left and right sides of the samples. Similarly, Li et al. [45] also pointed out the force increased rapidly, then bent resulted with delamination and finally longitudinal fiber fractures at the self-contact stage. Lastly, the combination of fiber debonding, matrix cracking, delamination and fiber breakage was observed as the mode of failures in all crushed samples.

3.2 Crushing load efficiency

The initial peak load and the mean crushing load, which are references for the spring back values and the crush load stability, were shown in Fig. 8. The maximum initial load or load carrying capacity as 12.72 kN was obtained from GFRP samples having $\pm(70^\circ)$ fiber orientation while the minimum one is 3.32 kN of CFRP with $\pm(40^\circ)$ orientation. There was no regular tendency for intraply samples, but their values were in the range of combined materials as expected. The mean crushing load values of CFRP were increased by inclusion of glass fibers (GCFRP). The improvements for $\pm(40^\circ)$, $\pm(55^\circ)$ and $\pm(70^\circ)$ fiber orientations, respectively,

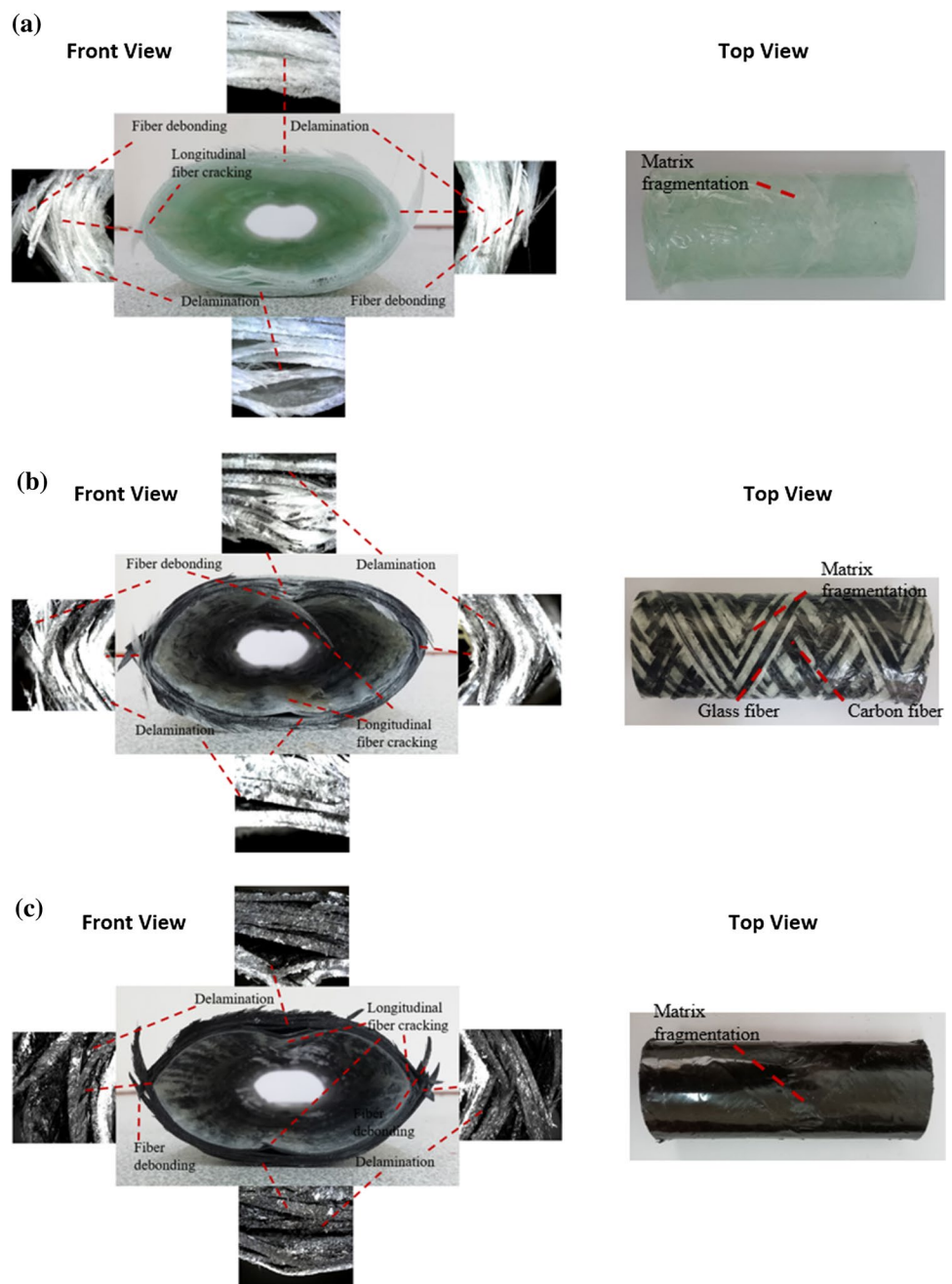
were 44.86%, 43.62%, 107.63% for glass fiber inclusion to carbon fiber (GCFRP).

The lateral crushing load efficiency values for FRP samples of $\pm(40^\circ)$, $\pm(55^\circ)$ and $\pm(70^\circ)$ fiber orientations were presented in Fig. 9, respectively. In general cases of the lateral crushing application especially for intraply hybridized samples, mean load was greater than the initial peak load values. Consequently, more than 100% load efficiency took place on the results. It can be said that higher fiber orientation angle resulted in decrease for crushing load efficiency for non-hybrid samples. This situation is suspected to be a consequence of the higher initial peak load compared to mean crushing load which led to progressive failures [40, 54]. Thus, it can be said that initial peak load values exhibited the higher increments than mean crushing loads as fiber orientation angle increased.

3.3 Energy absorption

Total absorption energy of the samples with different fiber orientation angles was presented in Fig. 10. GCFRP intraply samples had the behavior between the carbon and glass fiber-reinforced pipes as expected. The maximum total energy absorption by GFRP with $\pm(70^\circ)$ fiber orientation as 303.2 J. Due to fact that of crushing load of GFRP was much higher than CFRP counterparts at the crushing stage, the GFRP pipes absorbed more energy throughout the test. Similar results were also seen in a study of Li [45] in which it was

Fig. 7 Macro- and micro-damages of samples; **a** GFRP, **b** GCFRP, **c** CFRP

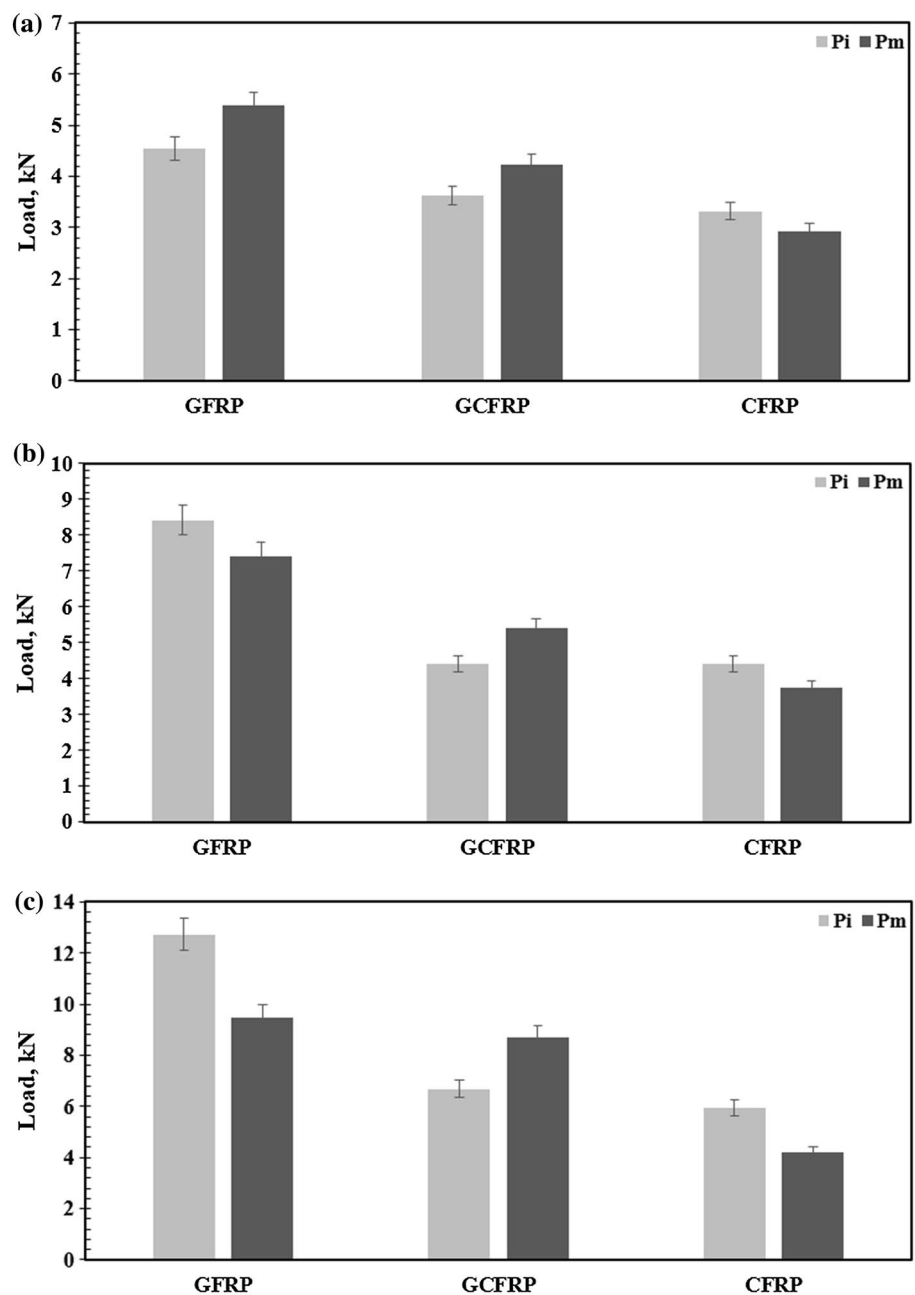


reported that although CFRP tubes dissipated more energy at the elastic region of load–displacement curves, GFRP tubes had the more energy absorption than CFRP owing to higher mean crushing load. The improvements in the glass fiber inclusion to carbon fiber (GCFRP) were 44.2%, 45.2% and 114.3% for $\pm(40^\circ)$, $\pm(55^\circ)$ and $\pm(70^\circ)$ fiber orientation angles.

The specific absorbed energy is a crucial and more reliable to understand crushing response of the samples

due to mass consideration. According to different fiber orientation angles, specific absorbed energy values of the all samples were given in Fig. 11. All intraply hybridized samples remained the values between combined materials. Also, hybridization process proved to show improvements by inclusion a fiber type to weaker one. GCFRP had the 1.15, 1.10 and 1.13 times higher values than CFRP for considered fiber orientation angles, so glass and carbon fiber combination gave the better material in this manner.

Fig. 8 Loading characteristics for **a** $\pm(40^\circ)_6$ fiber orientation, **b** $\pm(55^\circ)_6$ fiber orientation, **c** $\pm(70^\circ)_6$ fiber orientation



3.4 Effect of fiber orientation

The lateral crushing parameters such as initial peak load, mean load, crushing load efficiency, total energy absorption and specific energy absorption, of the laterally crushed samples were examined as indicated in previous sections. It could be found that the fiber orientation angle had a significant influence on all parameters. As angle increased, initial peak load, mean crushing load, total energy absorption and specific absorbed energy of the samples displayed the increase trend while the crush load efficiency showed the slightly decrease tendency especially for hybrid samples as expected [38]. The increase

in the spring back load values was 179.56%, 85.04%, 79.21%, for GFRP, GCFRP, CFRP, respectively. GFRP with a value of 2.66 J/g absorbed the maximum energy in specific consideration. Total energy absorption and the specific absorbed energy tend to gradually increase trend because of the approaching fiber orientation to loading direction which shows maximum strength.

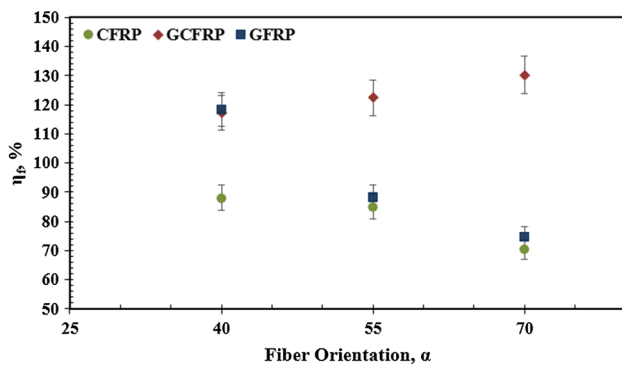


Fig. 9 Crushing load efficiency

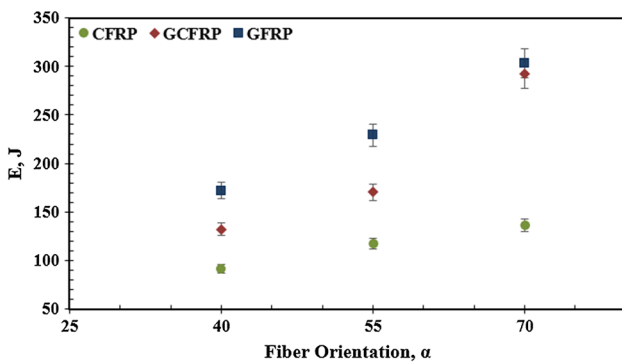


Fig. 10 Total energy absorption

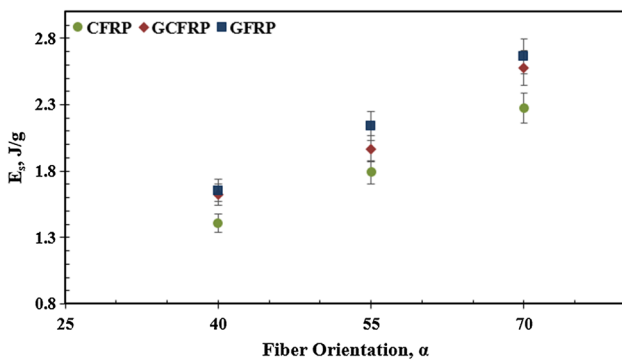


Fig. 11 Specific absorbed energy

4 Conclusions

In this study, the effects of the intraply fiber hybridization on the crashworthiness behaviors of the filament wound composite pipes subjected to lateral compression loading were experimentally investigated. The results obtained from the experiments can be summarized as follows:

- All samples responded the progressive failure history versus compression loadings. The separation between layers (delamination) after matrix fragmentation was seen as main damage mechanisms.
- The standard stable failure process as change in cross section from circular to elliptical was happened on all samples.
- The mean crushing load values and energy absorption capabilities of CFRP were increased by inclusion of glass fibers (GCFRP). Intraply samples proved to be excellent reformative characteristics on the weaker component of the pipes.
- GCFRP intraply samples, in terms of load carrying capacity, mean crushing load, energy absorption capability, had the behavior between the carbon and glass fiber-reinforced pipes as expected.
- Higher fiber orientation angle resulted in increase of initial peak load, mean crushing load and energy absorption capability. This situation was related to direction of the stronger component of the pipes approaching to loading axis.

In the view of above results, intraply fiber hybridization of carbon fiber with glass fiber provided improvements in the amount of absorbed energy compared to non-hybrid carbon fiber-reinforced composite pipe system.

References

1. Gemi L, Köklü U, Yazman Ş, Morkavuk S (2020) The effects of stacking sequence on drilling machinability of filament wound hybrid composite pipes: part-1 mechanical characterization and drilling tests. *Compos B Eng* 186:107787. <https://doi.org/10.1016/j.compositesb.2020.107787>
2. Prabhakar MM, Rajini N, Ayrilmis N, Mayandi K, Siengchin S, Senthilkumar K, Ismail SO (2019) An overview of burst, buckling, durability and corrosion analysis of lightweight FRP composite pipes and their applicability. *Compos Struct*. <https://doi.org/10.1016/j.compstruct.2019.111419>
3. Gemi L, Morkavuk S, Köklü U, Yazman Ş (2020) The effects of stacking sequence on drilling machinability of filament wound hybrid composite pipes: part-2 damage analysis and surface quality. *Compos Struct* 235:111737. <https://doi.org/10.1016/j.compstruct.2019.111737>
4. Yan L, Chouw N, Jayaraman K (2014) Lateral crushing of empty and polyurethane-foam filled natural flax fabric reinforced epoxy composite tubes. *Compos B Eng* 63:15–26. <https://doi.org/10.1016/j.compositesb.2014.03.013>
5. Bambach MR (2010) Axial capacity and crushing behavior of metal–fiber square tubes–steel, stainless steel and aluminum with CFRP. *Compos B Eng* 41(7):550–559. <https://doi.org/10.1016/j.compositesb.2010.06.002>
6. Mahdi E, Sebaey TA (2014) Crushing behavior of hybrid hexagonal/octagonal cellular composite system: aramid/carbon hybrid composite. *Mater Des* 63:6–13. <https://doi.org/10.1016/j.matdes.2014.06.001>

7. Gemi L (2018) Investigation of the effect of stacking sequence on low velocity impact response and damage formation in hybrid composite pipes under internal pressure. A comparative study. *Compos B Eng* 153:217–232. <https://doi.org/10.1016/j.compositesb.2018.07.056>
8. Rafiee R, Ghorbanhosseini A (2020) Developing a micro-macromechanical approach for evaluating long-term creep in composite cylinders. *Thin-Walled Struct* 151:106714. <https://doi.org/10.1016/j.tws.2020.106714>
9. Rafiee R, Habibagahi MR (2018) On the stiffness prediction of GFRP pipes subjected to transverse loading. *KSCE J Civ Eng* 22(11):4564–4572. <https://doi.org/10.1007/s12205-018-2003-5>
10. Rafiee R, Ghorbanhosseini A, Rezaee S (2019) Theoretical and numerical analyses of composite cylinders subjected to the low velocity impact. *Compos Struct* 226:111230. <https://doi.org/10.1016/j.compstruct.2019.111.230>
11. Gemi L, Aksoyulu C, Yazman Ş, Özkılıç YO, Arslan MH (2019) Experimental investigation of shear capacity and damage analysis of thinned end prefabricated concrete purlins strengthened by CFRP composite. *Compos Struct* 229:111399. <https://doi.org/10.1016/j.compstruct.2019.111399>
12. Madenci E, Özkılıç YO, Gemi L (2020) Experimental and theoretical investigation on flexure performance of pultruded GFRP composite beams with damage analyses. *Compos Struct*. <https://doi.org/10.1016/j.compstruct.2020.112162>
13. Özbek Ö, Bozkurt ÖY, Erklığ A (2020) Low velocity impact behaviors of basalt/epoxy reinforced composite laminates with different fiber orientations. *Turk J Eng* 4(4):197–202. <https://doi.org/10.31127/tuje.644025>
14. Hawa A, Majid MA, Afendi M, Marzuki HFA, Amin NAM, Mat F, Gibson AG (2016) Burst strength and impact behaviour of hydrothermally aged glass fibre/epoxy composite pipes. *Mater Des* 89:455–464. <https://doi.org/10.1016/j.matdes.2015.09.082>
15. Onder A, Sayman O, Dogan T, Tarakcioglu N (2009) Burst failure load of composite pressure vessels. *Compos Struct* 89(1):159–166. <https://doi.org/10.1016/j.compstruct.2008.06.021>
16. Rafiee R, Habibagahi MR (2018) Evaluating mechanical performance of GFRP pipes subjected to transverse loading. *Thin-Walled Struct* 131:347–359. <https://doi.org/10.1016/j.tws.2018.06.037>
17. Özbek Ö, Bozkurt ÖY (2019) Hoop tensile and compression behavior of glass-carbon intraply hybrid fiber reinforced filament wound composite pipes. *Mater Test* 61(8):763–769. <https://doi.org/10.3139/120.111395>
18. Demirci MT, Tarakcioglu N, Avci A, Erkendirici ÖF (2014) Fracture toughness of filament wound BFR and GFR arc shaped specimens with Charpy impact test method. *Compos B Eng* 66:7–14. <https://doi.org/10.1016/j.compositesb.2014.04.015>
19. McGregor CJ, Vaziri R, Poursartip A, Xiao X (2007) Simulation of progressive damage development in braided composite tubes under axial compression. *Compos A Appl Sci Manuf* 38(11):2247–2259. <https://doi.org/10.1016/j.compositesa.2006.10.007>
20. Gemi L, Tarakcioglu N, Akdemir A, Şahin ÖS (2009) Progressive fatigue failure behavior of glass/epoxy (± 75)₂ filament-wound pipes under pure internal pressure. *Mater Des* 30(10):4293–4298. <https://doi.org/10.1016/j.matdes.2009.04.025>
21. Kara M, Kırıcı M (2017) Effects of the number of fatigue cycles on the impact behavior of glass fiber/epoxy composite tubes. *Compos B Eng* 123:55–63. <https://doi.org/10.1016/j.compositesb.2017.04.021>
22. Huang Z, Zhang W, Qian X, Su Z, Pham DC, Sridhar N (2020) Fatigue behaviour and life prediction of filament wound CFRP pipes based on coupon tests. *Mar Struct* 72:102756. <https://doi.org/10.1016/j.marstruc.2020.102756>
23. Demirci MT (2020) Low velocity impact and fracture characterization of SiO₂ nanoparticles filled basalt fiber reinforced composite tubes. *J Compos Mater*. <https://doi.org/10.1177/0021998320915952>
24. Uyaner M, Kara M, Şahin A (2014) Fatigue behavior of filament wound E-glass/epoxy composite tubes damaged by low velocity impact. *Compos B Eng* 61:358–364. <https://doi.org/10.1016/j.compositesb.2013.06.039>
25. Gemi L, Kayrıncı M, Uludağ M, Gemi DS, Şahin ÖS (2018) Experimental and statistical analysis of low velocity impact response of filament wound composite pipes. *Compos B Eng* 149:38–48. <https://doi.org/10.1016/j.compositesb.2018.05.006>
26. Gemi L, Morkavuk S, Köklü U, Gemi DS (2019) An experimental study on the effects of various drill types on drilling performance of GFRP composite pipes and damage formation. *Compos B Eng* 172:186–194. <https://doi.org/10.1016/j.compositesb.2019.05.023>
27. Maleki S, Rafiee R, Hasannia A, Habibagahi MR (2019) Investigating the influence of delamination on the stiffness of composite pipes under compressive transverse loading using cohesive zone method. *Front Struct Civ Eng* 13(6):1316–1323. <https://doi.org/10.1007/s11709-019-0555-1>
28. Özbek Ö, Bozkurt ÖY, Erklığ A (2019) An experimental study on intraply fiber hybridization of filament wound composite pipes subjected to quasi-static compression loading. *Polym Test* 79:106082. <https://doi.org/10.1016/j.polymertesting.2019.106082>
29. Pol MH, Golshan NR (2019) Experimental investigation of parameters affected on behavior of composite tubes under quasi static and dynamic axial loading. *Compos B Eng* 163:471–486. <https://doi.org/10.1016/j.compositesb.2019.01.011>
30. Quanjin M, Rejab MRM, Idris MS, Hassan SA, Kumar NM (2019) Effect of winding angle on the quasi-static crushing behaviour of thin-walled carbon fibre-reinforced polymer tubes. *Polym Polym Compos*. <https://doi.org/10.1177/0967391119887571>
31. Elahi SA, Rouzegar J, Niknejad A, Assaee H (2017) Theoretical study of absorbed energy by empty and foam-filled composite tubes under lateral compression. *Thin-Walled Struct* 114:1–10. <https://doi.org/10.1016/j.tws.2017.01.029>
32. Elgalai AM, Mahdi E, Hamouda AMS, Sahari BS (2004) Crushing response of composite corrugated tubes to quasi-static axial loading. *Compos Struct* 66(1–4):665–671. <https://doi.org/10.1016/j.compstruct.2004.06.002>
33. Liu Q, Xing H, Ju Y, Ou Z, Li Q (2014) Quasi-static axial crushing and transverse bending of double hat shaped CFRP tubes. *Compos Struct* 117:1–11. <https://doi.org/10.1016/j.compstruct.2014.06.024>
34. Kalhor R, Case SW (2015) The effect of FRP thickness on energy absorption of metal-FRP square tubes subjected to axial compressive loading. *Compos Struct* 130:44–50. <https://doi.org/10.1016/j.compstruct.2015.04.009>
35. Hu D, Zhang C, Ma X, Song B (2016) Effect of fiber orientation on energy absorption characteristics of glass cloth/epoxy composite tubes under axial quasi-static and impact crushing condition. *Compos A Appl Sci Manuf* 90:489–501. <https://doi.org/10.1016/j.compositesa.2016.08.017>
36. Sebaey TA, Mahdi E, Shamseldin A, Eltai EO (2014) Crushing behavior of hybrid hexagonal/octagonal cellular composite system: all made of carbon fiber reinforced epoxy. *Mater Des* 60:556–562. <https://doi.org/10.1016/j.matdes.2014.04.044>
37. Abdewi EF, Sulaiman S, Hamouda AMS, Mahdi E (2008) Quasi-static axial and lateral crushing of radial corrugated composite tubes. *Thin-Walled Struct* 46(3):320–332. <https://doi.org/10.1016/j.tws.2007.07.018>
38. Ismail AE, Sahrom MF (2015) Lateral crushing energy absorption of cylindrical kenaf fiber reinforced composites. *Int J Appl Eng Res* 10(8):19277–19288

39. Ramakrishna S (1997) Microstructural design of composite materials for crashworthy structural applications. *Mater Des* 18(3):167–173. [https://doi.org/10.1016/S0261-3069\(97\)00098-8](https://doi.org/10.1016/S0261-3069(97)00098-8)
40. Liu Q, Xu X, Ma J, Wang J, Shi Y, Hui D (2017) Lateral crushing and bending responses of CFRP square tube filled with aluminum honeycomb. *Compos B Eng* 118:104–115. <https://doi.org/10.1016/j.compositesb.2017.03.021>
41. Niknejad A, Elahi SA, Liaghat GH (2012) Experimental investigation on the lateral compression in the foam-filled circular tubes. *Mater Des* 1980–2015(36):24–34. <https://doi.org/10.1016/j.matdes.2011.10.047>
42. Abosbaia AS, Mahdi E, Hamouda AMS, Sahari BB, Mokhtar AS (2005) Energy absorption capability of laterally loaded segmented composite tubes. *Compos Struct* 70(3):356–373. <https://doi.org/10.1016/j.compstruct.2004.08.039>
43. Sari M, Karakuzu R, Deniz ME, Icten BM (2012) Residual failure pressures and fatigue life of filament-wound composite pipes subjected to lateral impact. *J Compos Mater* 46(15):1787–1794. <https://doi.org/10.1177/0021998311425717>
44. Hafeez F, Almaskari F (2015) Experimental investigation of the scaling laws in laterally indented filament wound tubes supported with V shaped cradles. *Compos Struct* 126:265–284. <https://doi.org/10.1016/j.compstruct.2015.02.073>
45. Li S, Guo X, Li Q, Ruan D, Sun G (2020) On lateral compression of circular aluminum, CFRP and GFRP tubes. *Compos Struct* 232:111534. <https://doi.org/10.1016/j.compstruct.2019.111534>
46. Swolfs Y, Gorbatikh L, Verpoest I (2014) Fibre hybridisation in polymer composites: a review. *Compos A Appl Sci Manuf* 67:181–200. <https://doi.org/10.1016/j.compositesa.2014.08.027>
47. Ha SK, Kim SJ, Nasir SU, Han SC (2012) Design optimization and fabrication of a hybrid composite flywheel rotor. *Compos Struct* 94(11):3290–3299. <https://doi.org/10.1016/j.compstruct.2012.04.015>
48. Standard ASTM (1994) D2584-94. Test method for ignition loss of cured reinforced resins. West Conshohocken, PA
49. Standard ASTM (2011) D2412. Standard test method for determination of external loading characteristics of plastic pipe by parallel-plate loading. American Society for Testing and Materials, Philadelphia
50. Wang Y, Feng J, Wu J, Hu D (2016) Effects of fiber orientation and wall thickness on energy absorption characteristics of carbon-reinforced composite tubes under different loading conditions. *Compos Struct* 153:356–368. <https://doi.org/10.1016/j.compstruct.2016.06.033>
51. Quaresimin M, Ricotta M, Martello L, Mian S (2013) Energy absorption in composite laminates under impact loading. *Compos B Eng* 44(1):133–140. <https://doi.org/10.1016/j.compositesb.2012.06.020>
52. Schoeppner GA, Abrate S (2000) Delamination threshold loads for low velocity impact on composite laminates. *Compos A Appl Sci Manuf* 31(9):903–915. [https://doi.org/10.1016/S1359-835X\(00\)00061-0](https://doi.org/10.1016/S1359-835X(00)00061-0)
53. Almeida JHS Jr, Ribeiro ML, Tita V, Amico SC (2016) Damage and failure in carbon/epoxy filament wound composite tubes under external pressure: experimental and numerical approaches. *Mater Des* 96:431–438. <https://doi.org/10.1016/j.matdes.2016.02.054>
54. Othman A, Abdullah S, Ariffin AK, Mohamed NAN (2016) Investigating the crushing behavior of quasi-static oblique loading on polymeric foam filled pultruded composite square tubes. *Compos B Eng* 95:493–514. <https://doi.org/10.1016/j.compositesb.2016.04.027>

Publisher's Note Springer Nature remains neutral with regard to jurisdictional claims in published maps and institutional affiliations.